JNCS
Journal of Nepal Chemical Society
June/July 2022, Vol. 43, No. 1, 75-88
ISSN: 2091-0304 (print)
DOI: https://doi.org/10.3126/jncs.v43i1.46999
RESEARCH ARTICLE

Alkaloidsextract of *Alnusnepalensis* Bark as a Green Inhibitor for Mild Steel Corrosion in 1 M H_2SO_4 Solution

Kamala Dhakal[1], Dilip Singh Bohara[1], Biren Bahadur Bist[1], Hari Bhakta Oli[1], Sanjay Singh[1], Deval Prasad Bhattarai[1], Nabin Karki[2], Amar Prasad Yadav[3*]

[1]Amrit Campus, Tribhuvan University, 44600, Kathmandu, Nepal

[2]Bhaktapur Multiple Campus, Tribhuvan University, 44800, Kathmandu, Nepal

[3]Central Department of Chemistry, Tribhuvan University, 44618, Kathmandu, Nepal

*Corresponding author: amar2y@yahoo.com

Submitted: **12 June 2022**, Revised **23 June 2022**, Accepted **26 June 2022**

Abstract

Extraction of alkaloids from *Alnus nepalensis* bark has been successfully carried out and used as a green inhibitor for mild steel corrosion exposed to 1 M H_2SO_4 solution. Alkaloids have been tested by chemical, UV and FTIR spectroscopic methods. Corrosion inhibition was monitored by weight loss measurement and electrochemical methods (open circuit potential method and potentiodynamic polarization method). Weight loss measurement was employed to study the inhibitor concentration and immersion time effect. Similarly, the temperature effect on inhibition efficiency was also carried out by this method. The maximum corrosion inhibition efficiency observed for 1000 ppm solution for 3 h was 71.94 % at 25 °C. The OCP measurement revealed that alkaloids acted as a mixed type of inhibitor.Potentiodynamic polarization for 3 h immersed samples in the presence and absence of inhibitors was carried out. The corrosion current density was decreased with the increasing concentration. The maximum efficiency of immersed sample in 1000 ppm inhibitor solution was 78.48 %. The adsorption isotherm and thermodynamic parameters were calculated and the energy of activation (Ea) wasfound to be 71.41 kJ/mol. The positive value of enthalpy indicated that the reaction involves is endothermic.

Keywords: *Alnus nepalensis, Green inhibitor, Mild steel, Polarization,* thermodynamic *parameters, Weight loss*

Introduction

Mild steel (MS) is a well-known ferrous alloy with 0.15-0.30% C, 0.4% Si, 0.7-0.9% Mn, 0.04% S, 0.04% P and is an excellent material used in structural and construction applications. The affluent use of MS as construction materials is because of its outstanding mechanical properties, ease of fabrication, excellent weldability, and low purchasing cost [1, 2]. However, it has low corrosion resistance, especially in acidic environments [3]. MS is prone to corrosion whose avoidance process is very complicated and requires bearing the huge cost to overcome this effect [4]. It is estimated that the global cost of corrosion is equivalent to 3-4% of their gross domestic product (GDP) of which 15-35% could be saved using available corrosion practice [5-7]. Karki *et.al* calculated the loss of about 4.3% of national GDP due to corrosion in the context of Nepal [8].

Various protective measures are being taken to prevent the corrosion of which use of inhibitor is effective [9]. An inhibitor is a chemical substance which is added in a small concentration to a corrosive environment to decrease the corrosion rate. A small portion of inhibitors is added continuously

or intermittently to the cleaning solvents like pickling acids, acid stimulation fluids, cooling waters, and oil and gasoline line production streams to control corrosion [9]. Corrosion inhibitors are mostly used in the processing industries like acid pickling, acid cleaning, oil well acidizing, acid descaling, boilers, etc., because of their low cost and easy practice [9, 10]. Mineral acids of different concentrations are extensively employed in various industrial processes which result in corrosion. To protect the metals from an aggressive environment, many organic compounds having one or more heteroatoms on their chemical structure mainly nitrogen have been studied and employed as corrosion inhibitors [9, 11].

Corrosion inhibitors are either synthetic or natural chemicals. Corrosion inhibitors are added to reduce the corrosion rates of metallic and alloy materials in different media [6]. Corrosion scientists are not very satisfied in the uses of chemical inhibitors as they are not readily available, toxic, expensive, water-insoluble, and pollute the environment in their synthesis and application processes. The search for eco-friendly inhibitors is the major motiffor the use of natural products as environmentally friendly inhibitors [12]. Interest in synthetic compounds as corrosion inhibitor is diminishing and the used natural products as corrosion inhibitor as an alternative.

The natural products contain various chemical compositions which are biodegradable and do not contain heavy metals or other toxic compounds [13]. The inhibition performances of plant extract are related to their chemical composition which takes the form of alkaloids, flavonoids, polyphenol, tannins, nitrogen bases, phenolics, carbohydrates, protein as well as hydrolysis products, etc. [14, 15]. These metabolites usually bear polar functional group-containing nitrogen, sulfur, or oxygen as heteroatoms, as well as triple or double conjugate bonds which act as major absorption centers on the surface of the metal. The lone pair of electrons in heteroatoms or π-electrons in conjugate bonds is responsible for the formation of layers over steel materials [15, 16].

Hitherto there is no especial remark for the use of green inhibitor extracted form *Alnus nepalensis*. Research reports have showed the presence of many important phytochemical constituents like flavonoids, alkaloids, phenolic compounds, amino acids, etc.,in this plant. Chemical constituents like 1,7-bis-(3,4-dihydroxyphenyl)-hexane-3-one-5-O-β-D xylopyranoside {oregonin}, taraxerone, taraxerol, betulin, beutilic acid, lupeol and β-sitosterol in the bark of *Alnusnepalensis* [17], and alkaloids like 2-Amino-4-oxo-3,4-dihydro-pteridine-6-carboxylic acid (1), (3-nitorpyridin-2-ylsulfanyl)-acetic acid (2), (6-cyano-5-methoxycarbonylmethyl-5,6-dimethyl-2-thioxo-piperidine-3-yl)-propionic acid methyl ester (3), and camptothecin (4), in the *Alnus nepalensis* bark are reported [18,19].

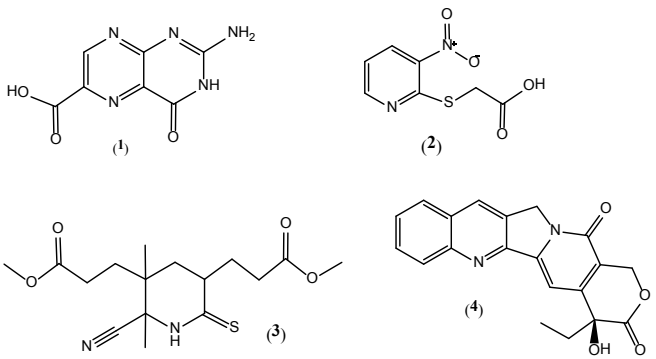

Scheme 1: Alkaloids reported in Alnus nepalensis species

Every phytochemical may have a role in corrosion inhibition but this study mainly focuses on the alkaloids because of the presence of nitrogen as heteroatom in the structure. In addition to carbon, hydrogen, and nitrogen, alkaloids may also contain oxygen, sulfur, and more rarely, other elements such as chlorine, bromine, and phosphorus [16]. The inhibition action could beattributed dueto the adsorption of the alkaloid molecules on the MS surface.

Materials and Methods

Extraction of Alkaloid from *Alnus nepalensis* bark

The bark of *Alnusnepalensis* was collected from Belkotgadi (Latitude: 27°83'21", longitude: 85°15'93", and altitude: 1050 m), Nuwakot, Bagmati Province, Nepal. The collected sample was shade dried, and ground into the fine powder. 100 g

of powder was soaked in hexane for 24 hours and filtered. The residue was then subjected to 700 mL of methanol for 7 days followed by filtration. The process was repeated until the colourless effluent was obtained. The filtrate was acidified using 5% tartaric acid, filtered and ammonia was added to maintain pH>10.Alkaloids (1°, 2°, and 3°) were separated in chloroform, it was concentrated using IKA RV 10 digital rotatory evaporator, and then dried in a water bath to get a solid residue named *Alnus nepalensis* alkaloid (ANA).

Chemical Test of ANA

To confirm the ANA, qualitative chemical tests and spectroscopic tests were performed. In the chemical method, Mayer's, Dragondroff's, and Wagner's testsas well as other phytochemical tests were performed.

UV-Vis and FTIR Spectroscopic Analysis of ANA

The spectroscopic characterization of ANA was performed using a Labtronics, LT-2802 double beam ultraviolet-visible (UV-Vis) spectrometer and PerkinElmer Spectrum IR Version 10.6.2 Fourier transform infrared (FTIR) spectrometer. FTIR data of solid ANA were collected in attenuated total reflectance (ATR) mode.The UV-Vis data were recorded by dissolving ANA in both aqueous and methanol.

Preparation of corrosive medium and inhibitor solution

A corrosive solution (1M H_2SO_4) was prepared by diluting appropriate volume of concentrated sulphuric acid (Fischer Scientific, India, sp. gravity 1.835, 97% purity) in a 1000 mL volumetric flask containing distilled water, and distilled water added up to mark. This solution was taken as corrosive media and used while analysing the weight loss and polarization measurement.

For the preparation of inhibitor solution, 1 g of ANA was dissolved in 1000 mL of 1 M H_2SO_4. A standard filter paper was used for filtration to remove undissolved ANA residue and volume maintained up to mark. The filtrate was labelled as an ANA stock solution of 1000 ppm. The working solutions of different concentrations (200, 400, 600, and 800 ppm) were prepared by serial dilution.

Preparation of mild steel (MS) sample

Mild steel (MS) samples of dimension (4×4×0.15) cm^3 were cut from a flat sheet collected from Banasthali, Kathmandu. Each coupon was abraded with silicon carbide (SiC) papers of the grits #100 to 1200. To remove residual particle, the abraded samples were washed with hexane and cleaned ultrasonically in ethanol. The surface area of each coupon was measured using a digital Vernier calliper before carrying out each experiment.

Weight Loss Measurement

The effect of immersion time, the effect of inhibitor concentration on corrosive media, and the effect of temperature for MS corrosion were studied by weight loss measurement method. The weight of MS coupons before and after immersion was measured by using an electronic balance (PH2204C). The weight loss measurements were carried out by dipping MS coupons in 100 mL 1 M H_2SO_4 and working solutions of different concentrations separately for the different time intervals of 0.5, 1, 3, 6, 18, and 24 h. The effect of temperature on inhibition efficiency and thermodynamic parameters were evaluated by taking measurements at 298, 308, 318, and 328 K using 200, 600, and 1000 ppm ANA solutions. The temperature was adjusted using a Clifton water bath (Model NE2-4D) for 1 h immersion time.

The difference in weight of the coupon before and after immersion was used to calculate the corrosion rate (mm/y), inhibitor efficiency (IE%), and surface coverage (Θ) using the formula in equations (1), (2), and (3) respectively.

$$\text{Corrosion rate (mm/y)} = \frac{K \times \Delta W}{A \times T \times D} \quad \ldots (1)$$

$$\text{Inhibition efficiency (IE\%)} = \frac{W_a - W_p}{W_a} \quad \ldots (2)$$

$$\text{Surface coverage } (\theta) = \frac{W_a - W_p}{W_a} \quad \ldots (3)$$

Where, K = constant = 87600
ΔW = weight loss in gram

A = Total surface area of mild steel in cm^2
T = Immersion time in the hour

D = Density of mild steel in g/cm^3
Wa and Wp are the weight loss values in the absence and presence of inhibitors, respectively.

Electrochemical Measurements

The electrochemical measurement was carried out using Hokuto Denko potentiostat (HA151, Japan). Measurement was carried out in a three-electrode system for which the mild steel coupon was used as a working electrode, graphite as a counter electrode, and a saturated calomel electrode (SCE) as a reference electrode. A small area (1 cm^2) of the MS coupons was exposed to 30 mL ANA solution as compared to that of the counter electrode (10cm^2) to exert uniform potential on the working electrode. A salt bridge was made to connect the working electrode to the SCE. A time interval of 30 minutes before polarization was given for each experiment to attain the steady-state open circuit potential (OCP). Then the sample was subjected to potentiodynamic polarization in the potential window ±0.35V from OCP with a scan rate of 1 mV/s, polarization starting from cathodic to the anodic limit. Polarization measurement was carried out in acid and for all concentrations of working solutions in 3 h immersed conditions. From the polarization curves, Tafel slope, corrosion potential, and corrosion current were estimated to evaluate the inhibition efficiency of ANA on MS corrosion in 1 M H_2SO_4, using the formula in equation (4).

$$\text{Corrosion Inhibition Efficiency (\%)} = \frac{I_{corr} - I^*_{corr}}{I_{corr}} \times 100 \quad \ldots (4)$$

Where, I_{corr} = corrosion current in absence of inhibitor
I^*_{corr} = corrosion current in the presence of inhibitor.

Results and Discussion

Chemical Test of ANA

A qualitative test for the confirmation of ANA was performed using three different tests. All the tests gave positive results that conform to the ANA. Findings are tabulated in table 1. ANA did not give +ve result for other phytochemical test. The possible chemical reaction of camptothecin molecule with the respective reagents is given in scheme 2 [20].

Table 1: Phytochemical screening of the extract solution

S.N.	Experiment	Observation	Result
1.	Mayer's Test	The appearance of an orange precipitate.	+ve
2.	Dragendroff 's Test	The appearance of orange-red color.	+ve
3.	Wagner's Test	The appearance of a reddish-brown precipitate.	+ve

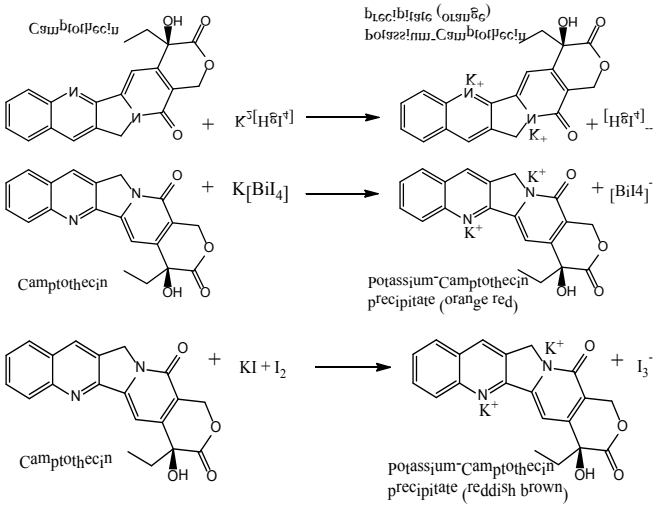

Scheme 2: Possible chemical reactions involved in the chemical test of ANA

UV-Vis and FTIR Spectroscopic Analysis of ANA

In the UV spectra (Figure 1), the sharp peak at 337 nm and 427 nm indicates the presence of lone pair of electrons and the unsaturation in the compound. The sharp peak at 337 nm is due to n-π* transition whereas the sharp peak at 427 is due to π-π* transition of electron in the ANA [18]. These two sharp peaks may indicate the presence of an aromatic ring containing N as heteroelement and the polyphenolic group in the structure (e.g. camptothecin).

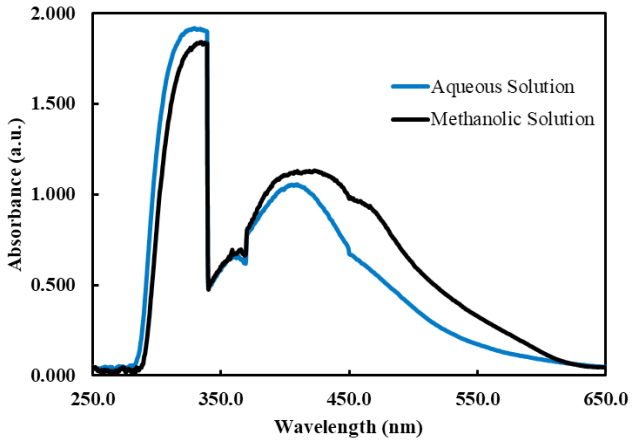

Figure 1: UV-Visible spectrum of methanol extract of *A. nepalensis*

FTIR spectroscopic analysis is a powerful tool that can be used to identify the type of bonding, π-bond conjugate system, aromatic and aliphatic structures, and particularly the functional group present in the organic compounds. It is also used to identify the carbon-heteroatom bond from their stretching frequency in the FTIR spectrum. In the spectrum (Figure 2), the peak around 3350 cm^{-1} is due to N-H stretching vibrations, a sharp peak at 2900 cm^{-1} is due to C-H stretching of the aromatic ring, a peak around 1232 cm^{-1} and 1024 cm^{-1} is due to C-N stretching of amines, and peak around 712 cm^{-1} is due to N-H bending vibration of primary and secondary amine [18].

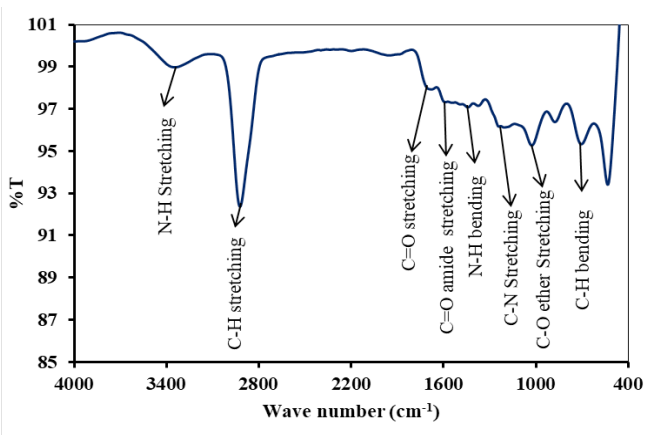

Figure 2: FTIR spectrum of ANA

Weight Loss Measurements

Effect of immersion time

The effect of immersion time for MS in 1 M sulphuric acid solution was studied by performing weight loss experiments in different time intervals (i.e., 0.5, 1, 3, 6, 18, and 24 h) in the presence and absence of inhibitor. The triplicate measurements on the weight loss of MS coupons were performed and expressed in g/cm^2 (Table 2). The weight loss of MS in acid only is very high in comparison to that in inhibitor solutions. Though there is weight loss in presence of inhibitor solution but the weight loss is very small. This decrease in weight loss is due to inhibition by ANA inhibitor.

Table 2: Variation of weight loss (g/cm^2) with different immersion time at different concentrations of inhibitors

Time (h)	Acid	200 ppm	400 ppm	600 ppm	800 ppm	1000 ppm
0.5	*0.000694*	*0.000518*	*0.000427*	*0.000349*	*0.000314*	*0.000233*
1	*0.002443*	*0.001811*	*0.001547*	*0.001191*	*0.001027*	*0.000767*
3	*0.011702*	*0.008293*	*0.007473*	*0.005736*	*0.00499*	*0.003284*
6	*0.023252*	*0.016566*	*0.014181*	*0.012493*	*0.009482*	*0.008063*
18	*0.061981*	*0.048643*	*0.041690*	*0.036487*	*0.034344*	*0.027791*
24	*0.073173*	*0.059112*	*0.050419*	*0.043272*	*0.04234*	*0.036187*

Weight loss of MS for half an hour immersion time was very small but on increasing immersion time, the weight loss in all the cases increases. As in Figure 3, the weight loss of the MS coupons was found highest in acid solution and the lowest in presence of 1000 ppm ANA solution.

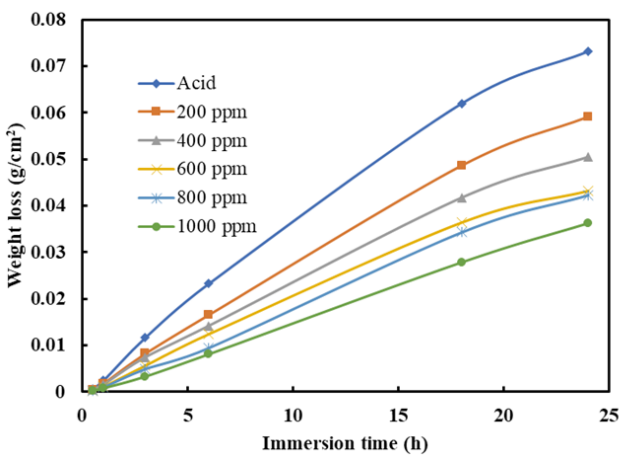

Figure 3: Variation of weight loss with immersion time for the corrosion of mild steel in the solution of 1M H_2SO_4 and ANA solution of different concentrations.

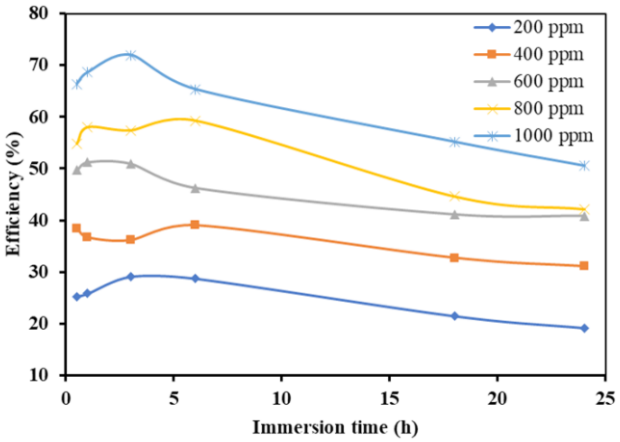

Figure 4: Variation of inhibition efficiency of different inhibitor solutions in 1M H_2SO_4 solution vs. time for the corrosion of mild steel at various times.

The inhibition efficiency of the inhibitor molecules of different concentrations in 1 M H_2SO_4 for MS samples is shown in Figure 4. It is observed that the inhibition of the inhibitor is very good at 1-6 h of immersion time. The maximum inhibition efficiency is found to be 71.94 % of 1000 ppm solution at 3 h immersion time. The inhibition efficiency increases up to 3 hours of immersion. However, with a prolonged immersion period there is a decrease in efficiency. This may be due to desorption of some of the adsorbed indicator molecules probably due to its bulky size and disrupted orientation in the realm of continuous attack of acid molecules from sides. It seems that IE of the inhibitor is less than 80% (i.e. maximum 66.38%) in short time of exposure. It means metal ions are dissolved in acid solution. These dissolved metal ions undergo chelation with inhibitor molecules forming chelate complex (Scheme 3). With increase in time, the availability of inhibitor molecules decreases resulting in the decrease in IE.

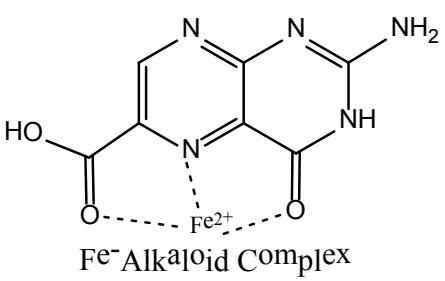

Scheme 3: *Fe-Alkaloid Complex*

Effect of ANA concentration

The decrease in weight of MS coupons dipped into acid solution is due to the formation of corrosion products. The weight loss of MS coupons also depends on the nature of the MS surface, temperature, and concentration of the inhibitor solution. The loss in weight of MS is very high in absence of an ANA inhibitor. Besides inhibitors, the loss in weight of MS gradually decreases with an increase in the concentration of ANA as shown in Figure 5. The minimum weight loss was observed in the 1000 ppm solution for 3 hours of immersion.

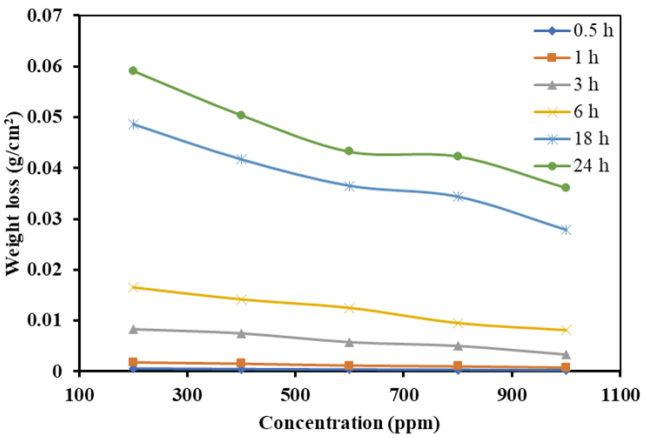

Figure 5: Variation of weight loss of MS in 1 M H_2SO_4 solution and ANA solutions at different time.

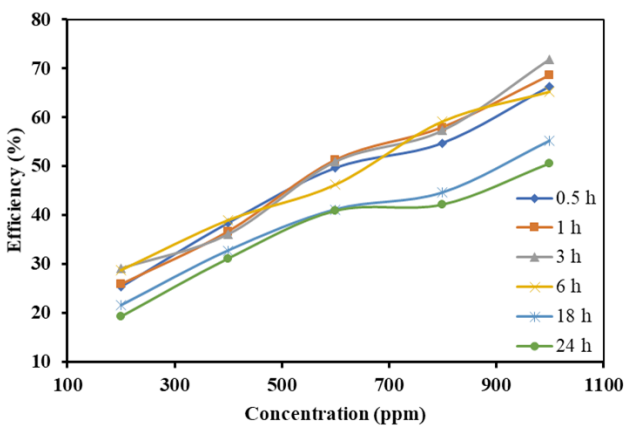

Figure 6: Inhibition efficiency of ANA in 1 M H_2SO_4 solution at different time

The inhibition efficiency of ANA solution of different concentrationsis presented in Figure 6. The inhibition efficiency of 200 and 400 ppm inhibitor concentrationsis almost negligible (less than 30% and 40%, respectively) and can be explained in the way that these concentrations are not sufficient to cover

the whole area of MS. Similarly, the 600 and 800 ppm inhibitor concentrations moderately inhibit the MS surface from an aggressive environment. However, the inhibition by 1000 ppm inhibitor solution is 71.94% at 3 h immersion time and is more than 60% up to 6 h of immersion time.This indicates that the 1000 ppm inhibitor solution can act as a good inhibitor up to 6 h of immersion time, but beyond this, the inhibition is not less than 50% which is also quite acceptable.

Adsorption Isotherm

This is a well-known fact that when solid substances are immersed in solutions, molecules from the solution get adsorbed on the solid surface. For a clear explanation of this adsorption process, it is better to know the adsorption isotherm.To identify the adsorption isotherm, Langmuir, Freundlich, and Tempkin adsorption isotherms were determined. All the molecules in ANA may not follow this trend, however, camptothecin (Structure **(4)** in Scheme 1, molecular weight 348.4) molecule is taken as reference to calculate the molar concentration of inhibitor solution. Langmuir's adsorption isotherm equation can be applied to find whether the adsorption process is monolayer or multilayer [21, 22]. The linear relation between the fraction of covered surface (θ) and molar concentration (C) should be known to find the adsorption isotherm. If the slope of the curve obtained by plotting $\frac{C}{\theta}$ vs C in equation (5) is unity then it indicates the monolayer adsorption,

$$\frac{C}{\theta} = \frac{1}{K} + C \quad \ldots (5)$$

Data obtained from 1 hour immersed sample were plotted between $\frac{C}{\theta}$ vs C,a straight line with a slope equal to 0.8286 is obtained (Table 3). This value has deviated from unity indicating both monolayer and multilayer adsorption of ANA on MS surface. It also indicates that multilayer formation onsets before the completion of monolayer adsorption. The formation of multilayer adsorption implies that there is a strong interaction between adsorbed layers which is further confirmed by two isotherms below. The value of slope and R^2 got deviated from unity (Figure 7), so that; the adsorption process in this corrosion inhibition process cannot be explained only by theLangmuir adsorption isotherm [21, 22].

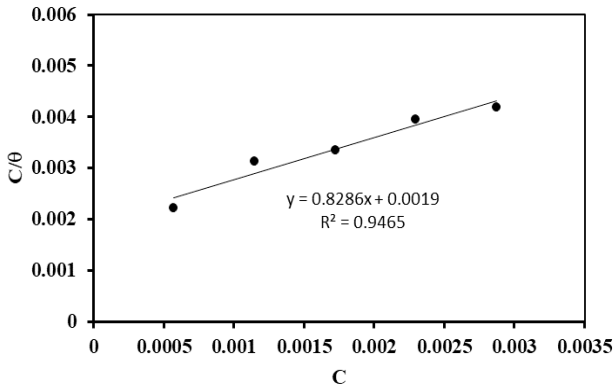

Figure 7: Langmuir adsorption isotherm plot for MS in 1 M H_2SO_4 with different concentrations of camptothecin

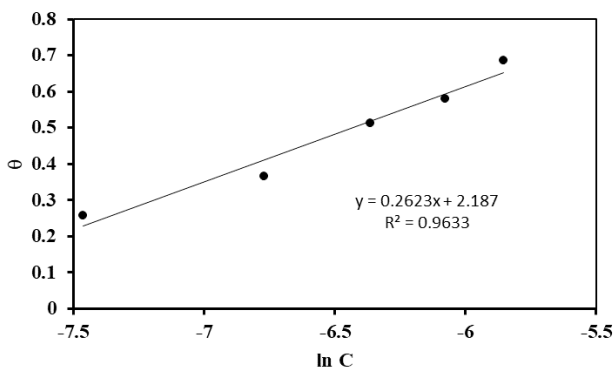

Figure 8: Temkin adsorption isotherm plot for MS in 1 M H_2SO_4 with different concentrations of camptothecin

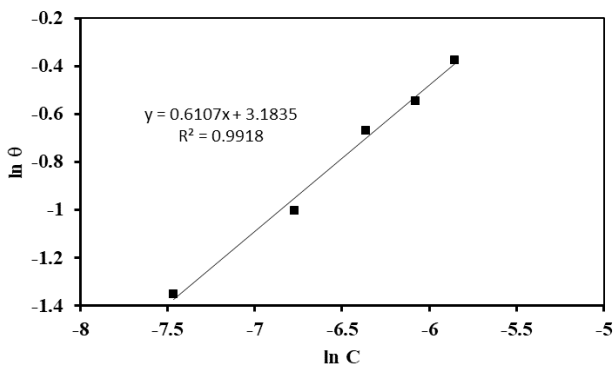

Figure 9: Freundlich adsorption isotherm plot for MS in 1 M H_2SO_4 solution with different concentrations ofcamptothecin

Temkin adsorption isotherm in equation (6) has been checked by plotting a graph ofθ against ln C where slope of 0.2623 and R^2 value of 0.9633 were obtained (Table 3).

$$\ln \theta = lnK + \frac{1}{n} \ln C \quad \ldots (6)$$

From the slope of the straight line in figure 8, the molecular interaction parameter (a) is calculated and found to be negative 1.90 indicating a strong attraction taking place in the adsorbed layer [22]. The value of K from the intercept is calculated and found 0.000239 indicating ANAs are strongly absorbed on the MS surface.

From the linear form of Freundlich adsorption isotherm equation (7), a curve between lnθ vs ln C is plotted as in figure 9. The R^2 value of the straight line is 0.9918, with a slope value (1/n) equal to 0.6107 which is in between 0<1/n<1 indicating the adsorption process is easy [22].

$$\ln \theta = lnK + \frac{1}{n} \ln C \quad \ldots (7)$$

The R^2 value gives the correlation between the measured values and hence helps to check the linearity range and hence the acceptability of the measured. There are three different R^2 values listed in table 3 for three different isotherms, namely; Langmuir adsorption isotherm, Temkin adsorption isotherm and Freundlich adsorption isotherm. Among them, the R^2 value for Langmuir isotherm deviates from unity whereas it is nearer to unity for Temkin isotherm. The R^2 value is 0.9918 for Freundlich adsorption isotherm and hence it is highly acceptable. The data are not strongly fitted for Langmuir adsorption isotherm, but Gibb's free energy has been calculated and found to be – 25.48 kJ/mol. It is clear from this value that the adsorption of ANA on MS surface is due to physical adsorption which will be further confirmed from thermodynamic parameters and electrochemical studies.

Table 3: Different parameters obtained from three different adsorption isotherms

Isotherm	Plotting	Slope	Intercept	R^2
Langmuir	C/θvs C	0.8286	0.0019	0.9465
Temkin	θvsln C	0.2623	2.187	0.9633
Freundlich	lnθvsln C	0.6107	3.1835	0.9918

Effect of temperature

The effect of temperature on the inhibition process was studied using the ANA solution of three different concentrations: 200, 600, and 1000 ppm. The weight loss measurement in these three different solutions at 25, 35, 45, and 55 °C, was measured taking reference tothe acid solution. For this measurement, the MS coupons were immersed in these solutions for one hour at mentioned temperature.

The weight loss of MS is maximum in acid solution and minimum at 1000 ppm inhibitor solution. The weight loss of MS in ANA solutions gradually got increased with increasing temperature. This increase in weight loss may be due to the desorption of the ANAs from the MS surface or may be due to the structural deformation of the ANAs [21]. The increase in weight loss leads to a decrease in inhibition efficiency of the ANA. The graph obtained by plotting weight loss per unit area per hour shows that there is small weight loss at low temperature but on increasing temperature the weight loss increases as shown in figure 10.

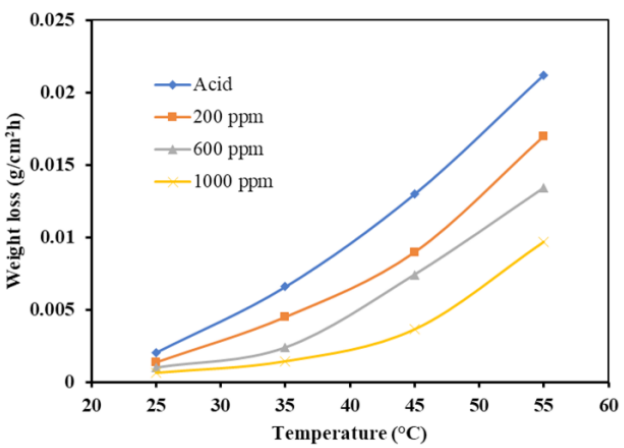

Figure 10: Variation of weight loss of mild steel coupons in 1 M H_2SO_4 and 200, 600, and 1000 ppm inhibitor at different temperatures.

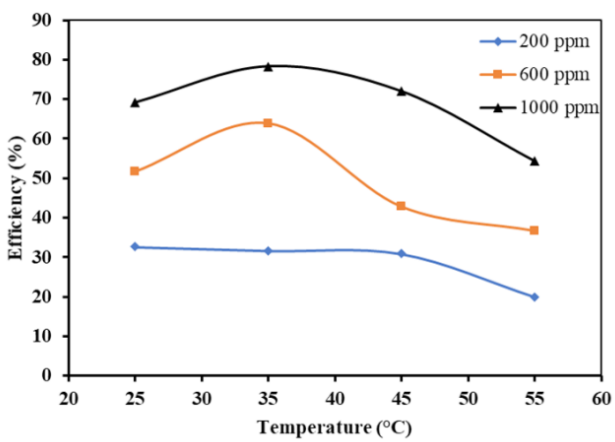

Figure 11: Variation of inhibition efficiency with temperature on the MS in presence of 200, 600, and 1000 ppm ANA in 1 M H_2SO_4 solution.

Figure 11 shows the variation of inhibition efficiency with temperature. It is clear from the figure that the 200 ppm inhibitor solution is almost inefficient for corrosion inhibition at every temperature. And the 600 ppm inhibitor solution showed good inhibition of corrosion at 35 °C. The inhibition efficiency of 1000 ppm inhibitor solution is almost good and linear up to 45 °C after which it gets declined. From these results, it can be concluded that desorption as well as the structural deformation of molecules may occur more at higher temperature. This deformation leads to the decrease in inhibition efficiency of the ANAs.

Activation energy and thermodynamic parameters

The activation energy of the reaction in the presence and absence of an inhibitor in an electrochemical cell can be explained by rearranging the Arrhenius equation [23]. The activation energy of the reaction is related to corrosion rate as,

$$\frac{1}{2.303RT} \quad (8)$$

Where A is the Arrhenius pre-exponential constant, T is the absolute temperature. Equation (8) reveals that the activation energy of the reaction is equal to the slope of the Arrhenius plot i.e. a plot obtained between logarithms of corrosion rate with $\frac{1}{2.303RT}$ along axes.

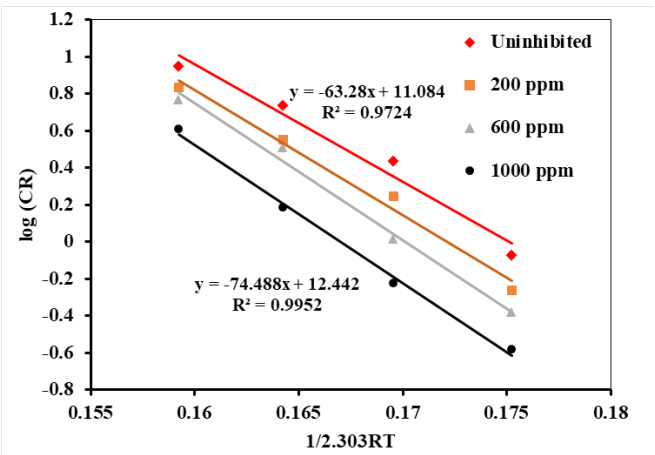

Figure 12: Arrhenius plot for MS in 1M H_2SO_4 with and without ANA

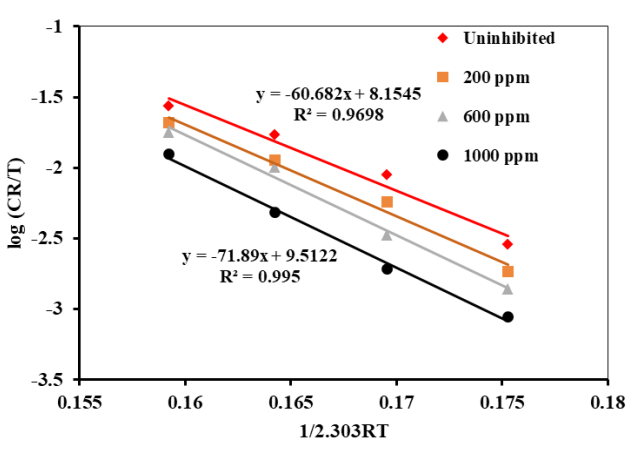

Figure 13: Transition state plot for MS in 1M H_2SO_4 with and without ANA

Arrhenius plot (Figure 12) shows that the energy of activation of the reaction between MS and acid in absence of an inhibitor is 63.20 kJ/mol. In addition to 200, 600, and 1000 ppm inhibitor, the activation energy increases to 67.53, 73.96, and 74.48 kJ/mol, respectively as shown in Table 4. This increase in activation energy reveals that with the addition of an inhibitor, inhibitor molecules suppress the reaction rate between acid and MS resulting in a decrease in corrosion rate. These calculated values are intermediate values between physical (less than or equal to 20 kJ/mol) and chemical interactions (more than 80 kJ/mol). Therefore, the adsorption of alkaloids on MS surface in 1M H_2SO_4 solution involves chemical-dominated physical interaction [24].

Enthalpy and entropy of the system can be calculated by using the transition state equation [25], an alternative form of the Arrhenius equation,

$$\log\left(\frac{C.R.}{T}\right) \quad (9)$$

Where, h is plank's constant, 6.6261×10^{-34}Js, and N is the Avogadro's number,

6.0225×10^{23} mol^{-1}. Enthalpy of activation (ΔH^o) is obtained as the slope of a straight line by plotting $\log\left(\frac{C.R.}{T}\right)$ vs. $\frac{1}{2.303RT}$ in the equation and the entropy of activation (ΔS^o) can be calculated from its intercept.From the transition state plot (Figure 13), the enthalpy of the system in the absence and presence of an inhibitor is estimated as in Table 4.

The positive value of ΔH* for adsorption of inhibitor on MS surface indicates that the adsorption is an endothermic process. The gradual increase in the value of ΔH* from 60.68 to 71.89 kJ/mol including 64.93 and 71.36 kJ/mol for acid only and different concentrations of inhibitor solution indicates a decrease in the corrosion rate controlled by kinetic parameters of activation. The Ea value higher than that of ΔH* indicates the involvement of a gaseous reaction i.e. cathodic hydrogen evolution reaction, resulting in the decrease in total reaction volume. The values of E_a and ΔH* also confirm the adsorption of the alkaloid by both physical and chemical interactions [22, 24].

Calculated values of E_a, ΔH°, and ΔS° for acid without and with inhibitor are tabulated in Table 4. The activation energy of the system gotincreased with the addition of inhibitors of three different concentrations. An increase in activation energy reduces the reaction rate resulting in the suppression of corrosion rate. An increase in E_a with the addition of inhibitor shows the strong adsorption of inhibitor molecules on the metal surface with complete or nearly complete coverage so that acid molecules have the least or almost no chance to react with metal.

Table 4:Activation parameters of the MS dissolution in 1 M H_2SO_4 without and with inhibitor.

Electrolyte	A (g/cm^2)	E_a (kJ/mol)	ΔH° (kJ/mol)	ΔS° (J/mol/K)
1M H_2SO_4	11.084	63.20	60.68	-41.3827
1M H_2SO_4 + 200 ppm Inhibitor	11.625	67.53	64.93	-31.0165
1M H_2SO_4 + 600 ppm Inhibitor	12.58	73.96	71.36	-12.7271
1M H_2SO_4 + 1000 ppm Inhibitor	12.442	74.48	71.89	-15.3866

Similarly, the entropy of these systems has been calculated from the intercept of the transition state plot. A significant negative value of ΔS* in 1M H_2SO_4 indicates the decrease in disordering from solution to activated complex formation phase on MS surface, also labelled as the association step in the rate-determining step. In addition to inhibitor, ΔS* value increases as negative 31.02, 12.72, and 15.38 J^{-1} $mol^{-1}K$ for 200, 600, and 1000 ppm inhibitor solutions, respectively. This implies that the randomness increased in the transition state due to the replacement of water molecules with alkaloid molecules [24].

The slope of the straight lines is gradually changed indicating that the inhibition is due to the physical adsorption process and there is no change in the mechanism of corrosion inhibition. The detailed process of physical adsorption is explained under the mechanism of inhibition title.

Electrochemical Measurements

Open Circuit Potential (OCP) measurement

The variation of open circuit potential (OCP) of mild steel in 1 M H_2SO_4 was studied by monitoring the changes in corrosion potential with time. The OCP change of MS immersed in ANA of different concentrations (200, 400, 600, 800, 1000 ppm) in 1 M sulphuric acid solution for 30 minutes at room temperatures were measured with the help of three-electrode system. OCP measured in acid solution with ANA of different concentrations is shown in Figure 14. It reveals that there is a slight shifting of potential towards an increase in OCP towards positive potential in presence of ANA but less than 85mV. This indicates that ANA might act as a mixed type of inhibitor. The positive shifting of potential from OCP indicates the formation of a protective layer by ANAs in acid solution on the MS surface that limits the interaction of aggressive ions with the MS surface [24].

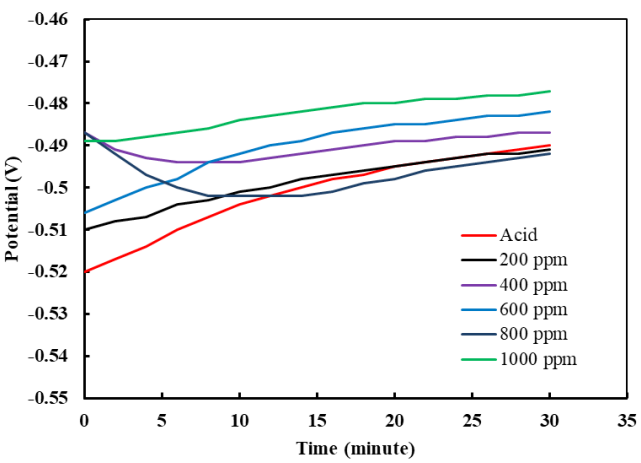

Figure 14: Variation of OCP with the immersion time of 3 h forMS coupons in different concentrations of ANA in 1M H_2SO_4.

Potentiodynamic Polarization Measurement

Potentiodynamic polarization measurement was carried out in a 3 h immersed sample. Figure 15 demonstrates the effect of ANA concentration (200, 400, 600, 800, and 1000 ppm) in 1 M H_2SO_4 solution on the polarization. The slight shifting of potential (<50 mV) in both anodic and cathodic directions indicates the mixed types of behavior of the inhibitors. It is found that the anodic slope is higher than the cathodic slope for the same concentration of acid and inhibitor solution. This is because of the dissolution of mild steel i.e. 1 mol of iron oxidation to ferrous ion releases two mol of electrons while reduction of one mol of hydrogen ion to hydrogen accepts one mol of electron at the same time. This results in the difference in anodic and cathodic slope. The current density gradually decreases from acid solution to 1000 ppm of inhibitor solution in one molar sulphuric acid. The decrease in current density implies that the inhibitor molecules highly resist on corrosion and minimizes the corrosion reaction.

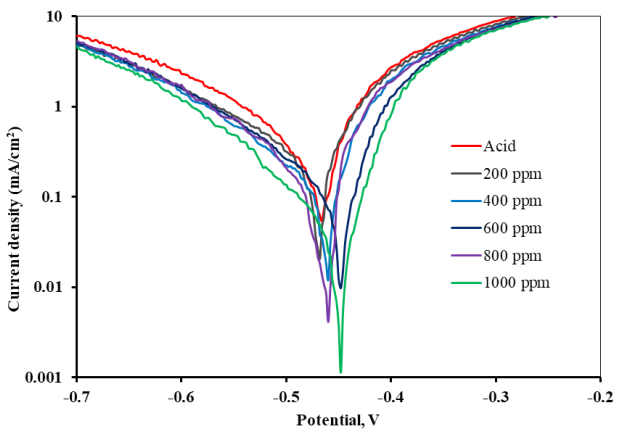

Figure 15: Potentiodynamic polarization curves for MS in 1M H_2SO_4 containing different concentrations of ANA in 3 h immersed condition.

The polarization curve also indicates that there is a decrease in current density with the addition of inhibitors. In the presence of an inhibitor, the MS surface is covered with inhibitor molecules so that the active site of MS is small. The reaction in this small area produces a small current density. This also indicates that the ANA used in this experiment is performing good inhibition. The inhibition efficiency, cathodic and anodic slope, corrosion potential, and corrosion current densities of the alkaloid are also tabulated in Table 5. The current density in acid-only solution is 0.12 A/cm^2 and the corrosion potential is 0.466 V. With the increased concentration of ANA, there is corresponding decrease in the current density. The minimum current density was observed at 1000 ppm inhibitor concentration (0.012A/cm^2) with a corrosion potential of 0.448V. This decrease in current density is due to the interaction of the ANA on the MS surface in the formation of a protective barrier with the reduction of active sites.

Table 5: Table showing the anodic slope, cathodic slope, and inhibition efficiency for 3 hours immersed sample

Medium	Ecorr	icorr	Anodic Slope	Cathodic Slope	Inhibition Efficiency (%)
Acid	0.466	0.120	28.6	12.6	-
200	0.468	0.064	25.3	9.3	46.67
400	0.460	0.042	26.3	7.1	65.00
600	0.448	0.034	24.3	6.4	71.67
800	0.460	0.026	29.8	7.6	78.33
1000	0.448	0.012	5.5	2.9	90.00

The inhibition efficiency of 200 ppm ANA solution is almost negligible whereas the inhibition by 400 ppm ANA solution is inan acceptable range. From this drastic change in the inhibition efficiency, it can be generalized that more than 400 ppm ANA concentration may be the effective concentration. To attain steady-state equilibrium between adsorbed and free inhibitor molecules, the inhibitor concentration plays an important role. After 400 ppm ANA concentration the inhibition gradually increases up to 1000 ppm concentration and inhibition reaches 90 %. This is because at higher concentration of inhibitor, ANAs can have sufficient concentration to get adsorbed and attain an equilibrium state [26]. This adsorbed layer protects the MS from an aggressive environment and reduces the corrosion rate. The detail efficiency variation is shown in Figure 16.

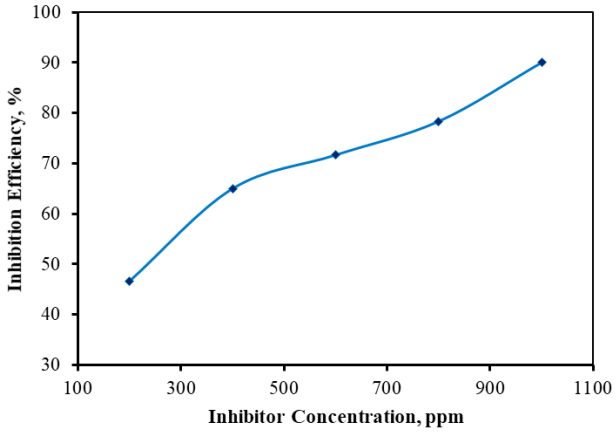

Figure 16: Inhibition efficiency of inhibitor obtained from the polarization of 3 hours immersed MS sample in 1 M H_2SO_4.

Mechanism of Corrosion Inhibition

The energy of activation (67.53 kJ/mol in 200 ppm, 73.96 kJ/mol in 600 ppm, and 74.48 kJ/mol in 1000 ppm inhibitor solution) reveals that there is physical adsorption between MS and alkaloid molecules. Corrosion inhibition by alkaloid molecules is due to the adsorption of inhibitor molecules on the MS surface by the replacement of water molecules, called the quasi-substitution process.

$$Org(sol) + xH_2O(ads) \rightleftharpoons Org(ads) + H_2O(sol)$$

Where Org(sol) and Org(ads) represent the solvated and adsorbed organic (alkaloid) molecules, respectively. Similarly, H_2O(ads) represents the adsorbed water molecules on the MS surface, and x represents the size ratio i.e. the number of water molecules that are replaced by one organic molecule [24].

OCP gives the information where there is a positively or negatively charged MS surface. The OCP of MS is recorded at around 0.49V. The shifting of OCP in presence of an indicator towards a more positive direction indicates that the MS surface is positively charged [26]. On a positively charged surface, there could be the interaction of SO_4^{2-} ions and the surface becomes negatively charged. Alkaloids contain mainly nitrogen as hetero element in the ring, which when dissolved in an acidic solution gets protonated. The protonated alkaloid molecules interact with sulfate ions by the electrostatic force of attraction. The protonated alkaloids return to their neutral form after releasing H_2 molecules [24, 26]. Then, electron pair of HOMO with high electron density of alkaloids especially the lone pair of nitrogen is shared with vacant d-orbital of iron forming co-ordinate covalent bond, which brings the accumulation of extra negative charge on metal surface. To relive the charge, electrons are returned to LUMO with high orbital density especially to antibonding π* orbital of organic molecule to form feedback bond. This retrodonation process strengthen the bond between MS and inhibitors. The steps of corrosion inhibition mechanism and schematic diagram (17) concerning camptothecin molecule are given as:

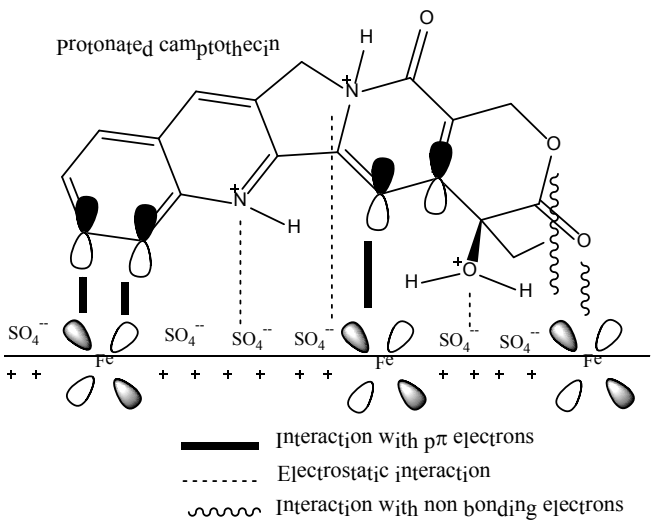

Figure 17: Schematic diagram for a different mode of adsorption of alkaloids on MS.

Conclusions

Extraction of ANA and its qualitative chemical test and spectrometric tests for its confirmation were carried out easily and successfully. Corrosion inhibition by ANA was determined by both weight loss and electrochemical methods. The maximum inhibition efficiency of 71.94% and 90% from the weight loss and polarization method, respectively, are investigated. Efficiency calculated from the electrochemical method can be regarded as more precise over those calculated from weight loss method as the instrumental methods owe less chance of handling error. All the results and discussion reveals that the corrosion inhibition is due to the formation of an adsorptive layer by ANA on the MS surface. The optimum concentration for the maximum inhibition

efficiency is 1000 ppm which had great inhibition efficiency up to 3 h. This extracted inhibitor can be used up to 45 °C temperature at which normal chemical cleaning processes are carried out. The extracted ANA can be used as a good inhibitor to control MS corrosion in the various industrial cleaning processes because of its promising efficiency.

Acknowledgments

The authors are thankful to the Department of Chemistry, Amrit Campus for laboratory support and the Central Department of Chemistry, Kirtipur for polarization measurements.

References

1. Shrestha, P. R., Oli, H. B., Thapa, B., Chaudhary, Y., Gupta, D. K., Das, A. K., Nakarmi, K. B., Singh, S., Karki, N., & Yadav, A. P. (2019). Bark extract of *Lantana camara* in 1M HCl as green corrosion inhibitor for mild steel. *Engineering Journal*, *23*(4), 205-211.
2. Yaro, A. S., Khadom, A. A., & Wael, R. K. (2013). Apricot juice as green corrosion inhibitor of mild steel in phosphoric acid. *Alexandria Engineering Journal*, *52*(1), 129-135.
3. Satapathy, A., Gunasekaran, G., Sahoo, S., Amit, K., & Rodrigues, P. (2009). Corrosion inhibition by *Justiciagendarussa* plant extract in hydrochloric acid solution. *Corrosion Science*, *51*(12), 2848-2856.
4. Ahmad, Z. (2006). *Principles of corrosion engineering and corrosion control*. Elsevier.
5. Koch, G., Varney, J., Thompson, N., Moghissi, O., Gould, M., & Payer, J. (2016). International measures of prevention, application, and economics of corrosion technologies study. *NACE international*, 216.
6. Adams, S., Aigbodion, V., Suleiman, I., &Momoh, I. (2019). Thermodynamic, Kinetic and Adsorptive Parameters of Corrosion Inhibition of Mild Steel Using *Polyalthialongifolia* Bark Extract in 0.5 M H_2SO_4. *International Journal of Science and Engineering Invention*, *5*(11), 1-7.
7. Al-Otaibi, M., Al-Mayouf, A., Khan, M., Mousa, A., Al-Mazroa, S., &Alkhathlan, H. (2014). Corrosion inhibitory action of some plant extracts on the corrosion of mild steel in acidic media. *Arabian Journal of Chemistry*, *7*(3), 340-346.
8. Karki, N. (2021). Development of green corrosion inhibitor for mild steel corrosion in acidic environment, A PhD thesis submitted to the Central Department of Chemistry, Tribhuvan University, Kathmandu, Nepal.
9. Al bahtiti, N & Abdel-Rahman, I. (2021). Anti-Corrosive Effect of Jordanian-Bay- Leaves Aqueous Extract on Mild Steel in 1.0 M Hydrochloric Acid Solution. *WSEAS Transactions on Environment and Development*. 17. 614-618. 10.37394/232015.2021.17.59.
10. Makhlouf, A. S. H. (2014). *Handbook of smart coatings for materials protection*. Elsevier.
11. Sastri, V. S. (1998). *Corrosion inhibitors: principles and applications*. Wiley New York.
12. Santana, C. A., Cunha, J. N. D., Rodrigues, J. G., Greco-Duarte, J., Freire, D. M., &D'Elia, E. (2020). Aqueous extracts of the castor beans as a corrosion inhibitor of mild steel in HCl media. *Journal of the Brazilian Chemical Society*, *31*, 1225-1238.
13. Ikeuba, A., Okafor, P., Ekpe, U., &Ebenso, E. E. (2013). Alkaloid and non-alkaloid ethanolic extracts from seeds of Garcinia kola as green corrosion inhibitors of mild steel in H_2SO_4 solution. *International Journal of Electrochemical Science*, *8*(5), 7455-7467.
14. Uwah, I., Okafor, P., & Ebiekpe, V. (2013). Inhibitive action of ethanol extracts from *Nauclealatifolia* on the corrosion of mild steel in H_2SO_4 solutions and their adsorption characteristics. *Arabian Journal of Chemistry*, *6*(3), 285-293.
15. Africa, S. (2008). Adsorption and inhibitive properties of ethanol extracts of *Musa sapientum* peels as a green corrosion inhibitor for mild steel in H_2SO_4. *African Journal of Pure and Applied Chemistry*, *2*(6), 046-054.

16. Thapa, B., Gupta, D. K., &Yadav, A. P. (2019). Corrosion inhibition of bark extract of *Euphorbia royleana* on mild steel in 1M HCl. *Journal of Nepal Chemical Society*, *40*, 25-29.

17. Son, P. T. (2008). Chemical constituents of the leaves of *Alnusnepalensis* D. Don. (Betulaceae). *Vietnam Journal of Chemistry*, *46*(4), 521.

18. R. M., Silverstein and F. X., Webster., *Spectrometric Identification of Organic Compounds*, 6th edition, John Wiley & Sons, Inc., USA, 2006, P. 99-106.

19. Rui, C. H. E. N., Ying-gang, L. U. O., Xiao-yu, H. U., Xiao-zhen, C. H. E. N., &Guo-lin, Z. H. A. N. G. (2008). Chemical Study on *Alnusnepalensis*. *Natural Product Research & Development, 20*(4).

20. Li, D., Zhang, P., Guo, X., Zhao, X., & Xu, Y. (2019). The inhibition of mild steel corrosion in 0.5 M H_2SO_4 solution by radish leaf extract. *Royal Society of Chemistry, 9*, 40997.

21. Andoor, P. A., Okeoma, K. B., &Mbamara, U. S. (2021). Adsorption and thermodynamic studies of the corrosion inhibition effect of Rosmarinusofficinalis L. leaves on aluminium alloy in 0.25 M HCl and effect of an external magnetic field. *International Journal of Physical Sciences*, *16*(2), 79-95.

22. Ituen, E., Akaranta, O., & James, A. (2017). Evaluation of performance of corrosion inhibitors using adsorption isotherm models: an overview. *Chem. Sci. Int. J*, *18*(1), 1-34.

23. Khalil, K. S. (2014). Corrosion inhibition of zinc in hydrochloric acid solution using ampicillin. Iraqi Journal of Science, 55(2).

24. Karki, N., Neupane, S., Gupta, D. K., Das, A. K., Singh, S., Koju, G. M., ...& Yadav, A. P. (2021). Berberine isolated from Mahonianepalensis as an eco-friendly and thermally stable corrosion inhibitor for mild steel in acid medium. *Arabian Journal of Chemistry*, *14*(12), 103423.

25. Karthik, R., Muthukrishnan, P., Chen, S. M., Jeyaprabha, B., & Prakash, P. (2015). Anti-corrosion inhibition of mild steel in 1M hydrochloric acid solution by using *Tiliacoraaccuminata* leaves extract. Int J ElectrochemSci, 10, 3707-3725.

26. Karki, N., Neupane, S., Chaudhary, Y., Gupta, D. K., & Yadav, A. P. (2021). Equisetum hyemale: a new candidate for green corrosion inhibitor family. *International Journal of Corrosion and Scale Inhibition*, *10*(1), 206-227.